MECSOL 2019 - Proceedings of the 7th International Symposium on Solid Mechanics
V. Tita, A. Ferreira, M.L. Ribeiro, A. Vieira and A.T. Beck (Editors), ABCM, Sao Carlos, SP, Brazil, April 15th to 17th, 2019

Correlation between physical wavenumbers and singularities in the integrand of Green's functions for layered media

I. Cavalcante and J. Labaki

School of Mechanical Engineering, University of Campinas, SP, Brazil

Abstract: This work investigates the issue of localization of singularities in the numerical integration of improper integrals of singular functions. Such integrals are common in many engineering problems that are solved with the aid of space transforms. Boundary element and other meshless methods that involve computing Green's functions are also examples of methods in which such integrals must be solved. A fundamental part of numerical integration schemes is the localization of the singularities on the path of integration, after which the singularities can be integrated. This work focuses on the case of Green's functions for a multilayered transversely isotropic half-space.
Keywords: numerical integration, singular integrands, Green's functions, localization of singularities

INTRODUCTION

This work is an extension of Azevedo, Cavalcante and Labaki's (2017) work, which considered the problem of numerical integration of singular improper integrals by locating the multiple singularities in the integrand by specifying their branch cuts, and their subsequent integration by a combination of analytical and numerical techniques. That work dealt with singular integration without being restricted to a specific application, although it provided a case study for a homogeneous, elastic half-space. In those cases, there are closed-form expressions for the values of the integration variable where the singularities lie.

In the present work, we address the case of Green's function for the vertical time-harmonic displacement response of a multilayered transversely isotropic half-space with an axisymmetric disc load on its surface. This response is obtained through a direct stiffness matrix superposition method (Wang and Rajapakse, 1994), in which the stiffness matrix of each layer in the system is superposed to form a stiffness matrix of the layered system, not unlike it is done with typical finite element codes. The stiffness matrix of each layer consists of Green's functions for soil media, which have been derived by Rajapakse and Wang (1993) in terms of Hankel transforms. These Green's functions are presented in terms of improper integrals and their integrands contain a number of singularities together with an oscillatory-decaying behavior. Due to the normalization of the integration interval proposed by Rajapakse and Wang (1993), all the singularities fall within a predictable interval. Differently than in the previous work by Azevedo et al. (2017), in this case there is no general closed-form solution for the location of the singularities in the integration path.

This work tackles the localization of singularities within the integration path of Green's functions for the aforementioned media. Localization of singularities is a necessary step in most integration methods. The results indicate that there is a direct connection between mathematical branch cuts in the integration path and physical wavenumbers of each layer.

STATEMENT OF THE PROBLEM

Consider a case of the time-harmonic displacement response of a transversely isotropic full-space containing a buried, axisymmetric disc load, the motion of which is described in cylindrical coordinates by the displacements u_i $(i = r,z)$ in the r and z directions, respectively. The cylindrical coordinates system is placed so that the z axis is orthogonal to the material's plane of isotropy, and the load is applied on the $x-y$ plane and centered at the origin. A solution for these displacement fields were obtained by Rajapakse and Wang (1993) through Hankel transforms and are given by:

$$u_i = \delta^2 \int_0^\infty u_i^* \zeta d\zeta, \quad i = r,z \tag{1}$$

where $\zeta = \lambda'/\delta$, in which λ' is the Hankel space variable and

$$u_r^* = a_1 A e^{-\delta\xi_1 z} + a_1 B e^{+\delta\xi_1 z} + a_2 C e^{-\delta\xi_2 z} + a_2 D e^{+\delta\xi_2 z} \tag{2}$$

$$u_z^* = -(a_7 A e^{-\delta\xi_1 z} - a_7 B e^{+\delta\xi_1 z} + a_8 C e^{-\delta\xi_2 z} - a_8 D e^{+\delta\xi_2 z}) \tag{3}$$

A, B, C and D are arbitrary functions that can be determined from the boundary and continuity conditions of a given problem. All other variables in Eqs. (2) and (3) are presented in the Appendix.

Figure 1 shows the behavior of the integrand, Eq. (3), within the region where the singularities occur, for the case of a homogeneous half-space under a vertical, unit disc load on its surface. The figure shows the influence of different damping factors in the behavior of the integrand.

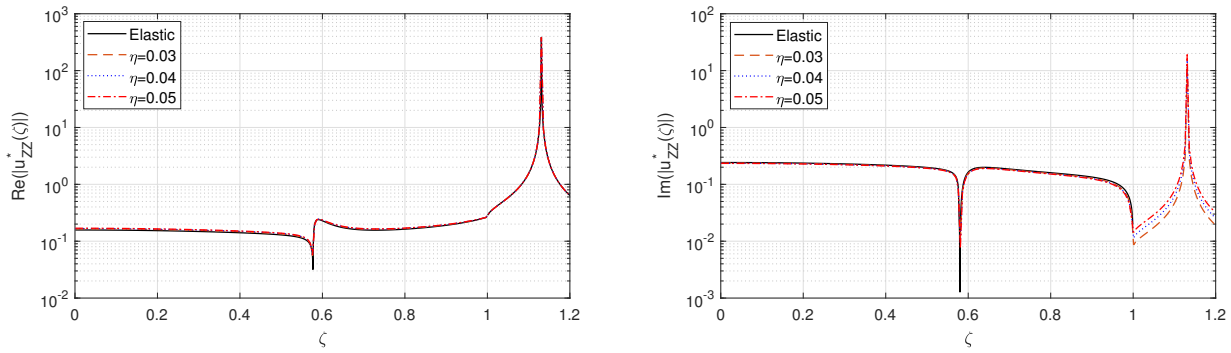

Figura 1 – Real and imaginary parts of u^*_{zz} for elastic and damped cases

The goal of this article is to find the location of the singularities such as shown in Fig. 1 for the case of multilayered half-spaces, as a necessary step for Eq. (1) to be integrated by an appropriate numerical scheme.

MULTILAYERED SOIL

A solution for the integrand in Eq. (1) for the case of a N-layered half-space (Fig. 2) has been derived by Labaki, Mesquita and Rajapakse (2014) from a general expression presented earlier by Rajapakse and Wang (1993). The radial and vertical displacements $u^*_i(z_n)$, $i = r,z$, $n = 1, N+1$ of the layer interfaces due to radial and vertical ring loads at arbitrary layers is given in the Hankel transformed domain by

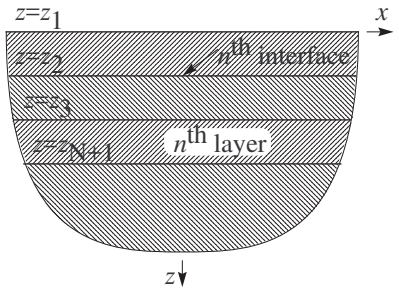

Figura 2 – Layered half-space with layer and interface numbering

$$\wp^* = Ku^* \tag{4}$$

in which

$$\wp^* = \left\langle \begin{array}{cccccc} \wp_r^{*1} & \wp_z^{*1} & \dots & \wp_r^{*(N+1)} & \wp_z^{*(N+1)} \end{array} \right\rangle^T \tag{5}$$

$$u^* = \left\langle \begin{array}{cccccc} u_r^*(r,z_1) & u_z^*(r,z_1) & \dots & u_r^*(r,z_{N+1}) & u_z^*(r,z_{N+1}) \end{array} \right\rangle^T \tag{6}$$

and

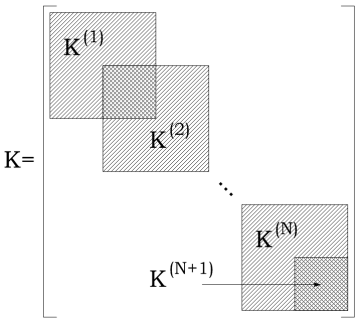

(7)

where $\wp^* = 1/\zeta s J_1(\zeta s)$ is a unit disc load of radius s described in the Hankel transformed domain.
The sections $K^{(n)}$ in Eq. (7) are the stiffness matrices of layer i, given by $K^{(n)} = F^{(n)}(G(n))^{-1}$, where

$$G^{(n)} = \begin{bmatrix} a_1 e_{1,n}^{-1} & a_1 e_{1,n}^{+1} & a_2 e_{2,n}^{-1} & a_2 e_{2,n}^{+1} \\ -a_7 e_{1,n}^{-1} & a_7 e_{1,n}^{+1} & -a_8 e_{2,n}^{-1} & -a_8 e_{2,n}^{+1} \\ a_1 e_{1,n+1}^{-1} & a_1 e_{1,n+1}^{+1} & a_2 e_{2,n+1}^{-1} & a_2 e_{2,n+1}^{+1} \\ -a_7 e_{1,n+1}^{-1} & a_7 e_{1,n+1}^{+1} & -a_8 e_{2,n+1}^{-1} & a_8 e_{2,n+1}^{+1} \end{bmatrix} \tag{8}$$

and

$$\frac{F^{(n)}}{c_{44}^{(n)}} = \begin{bmatrix} b_{51} e_{1,n}^{-1} & -b_{51} e_{1,n}^{+1} & b_{52} e_{2,n}^{-1} & -b_{52} e_{2,n}^{+1} \\ -b_{21} e_{1,n}^{-1} & -b_{21} e_{1,n}^{+1} & -b_{22} e_{2,n}^{-1} & -b_{22} e_{2,n}^{+1} \\ -b_{51} e_{1,n+1}^{-1} & b_{51} e_{1,n+1}^{+1} & -b_{52} e_{2,n+1}^{-1} & b_{52} e_{2,n+1}^{+1} \\ b_{21} e_{1,n+1}^{-1} & b_{21} e_{1,n+1}^{+1} & b_{22} e_{2,n+1}^{-1} & b_{22} e_{2,n+1}^{+1} \end{bmatrix} \tag{9}$$

for $n = 1, N$, and

$$G^{(N+1)} = \begin{bmatrix} a_1 e_{1,N+1}^{-1} & a_2 e_{2,N+1}^{-1} \\ -a_7 e_{1,N+1}^{-1} & -a_8 e_{2,N+1}^{-1} \end{bmatrix} \tag{10}$$

and

$$\frac{F^{(N+1)}}{c_{44}^{(n)}} = \begin{bmatrix} b_{51} e_{1,N+1}^{-1} & b_{52} e_{2,N+1}^{-1} \\ -b_{21} e_{1,N+1}^{-1} & -b_{22} e_{2,N+1}^{-1} \end{bmatrix} \tag{11}$$

for n=N+1 (half-space). In Eqs. (8) to (11), $e_{i,j}^{\pm 1} = e^{\pm \delta^{(n)} \xi_i^{(n)} z_j}$, $i = 1, 2$, $j = 1, N+1$. The other parameters involved in Eqs. (8) to (11) are shown in the Appendix.

LOCALIZATION OF SINGULARITIES

The Green's function describing a homogeneous half-space is characterized by three propagating elastic pressure and shear waves, the wavenumbers of which are, respectively, (Barros, 1996)

$$k_P = \pm\sqrt{1/\beta} \tag{12}$$

$$k_S = \pm 1 \tag{13}$$

and Rayleigh waves, the wavenumber of which are $k_R = k$ such that

$$[2(1-\kappa)k^2 - \gamma k^2 + \alpha](1-k^2) - \alpha\xi_1\xi_2 = 0 \tag{14}$$

Azevedo et al. (2017) have shown that the three singularities observed in the integrand of Eq. (1) correspond to each of these physical wave numbers: $\zeta_R = k_R$, $\zeta_P = k_P$, and $\zeta_S = k_S$ (Fig. 1). Finite layers within the layered system still

possess associated wavenumbers due to pressure, shear, and Rayleigh waves. Additionally, a singularity is observed in layered systems, which is given by

$$k_I = \frac{\sqrt{-1+\alpha+\kappa}}{\sqrt{-1+\alpha\beta+2\kappa-\kappa^2}}. \tag{15}$$

This singularity may or may not exist, depending on materials parameters of each layer. Their physical correlation and condition of existence require further investigation.

It is expected that the wavenumbers corresponding to each layer will correlate to each singularity in the integration path of the Green's function for the layered system. This is verified in the following section.

NUMERICAL RESULTS

The localization of singularities based on physical wavenumbers of the layered half-space is illustrated in this section with a representative example of one finite layer of thickness $h/s = 0.5$ over an unbound half-space. The material properties are $c_{44}^{(1)}/c_{44}^{(2)} = 3.125$, $\rho^{(1)}/\rho^{(2)} = 1.09086$, and $\nu^{(1)}/\nu^{(2)} = 0.7697$ (see Appendix), and $a_0 = s\omega(\rho^{(2)}/c_{44}^{(2)})^{(1/2)} = 0.3165$, in which the upper indices (1) and (2) indicate respectively the layer and the half-space.

For the parameters considered in this analysis, Eqs. (12) to (15) predict the occurence of singularities at $\zeta_P = 0.57735$, $\zeta_S = 1$, $\zeta_I = 0.707107$, and $\zeta_R = 1.008$ due to the wavenumbers corresponding to the top layer, and at $\zeta_P = 0.27537$, $\zeta_S = 1$, $\zeta_I = 0.34544$, and $\zeta_R = 1.008$ due to the wavenumbers corresponding to the half-space. There are, therefore, six different singularities in the integrand, at $\zeta' = 0.27537$, $\zeta' = 0.34544$, $\zeta' = 0.57735$, $\zeta' = 0.707107$, $\zeta' = 1$, and $\zeta' = 1.008$.

Figure 3 shows the real and imaginary parts of the integrand $u_z^*(\zeta)$ (Eq. (3)) at the surface of the layered half-space, $z/s = 0$, and at the interface between the layer and the half-space, $z/s = 0.5$. Notice that the coordinate r only comes into the integrand as an argument of the Bessel functions, therefore not affecting the location of the singularities.

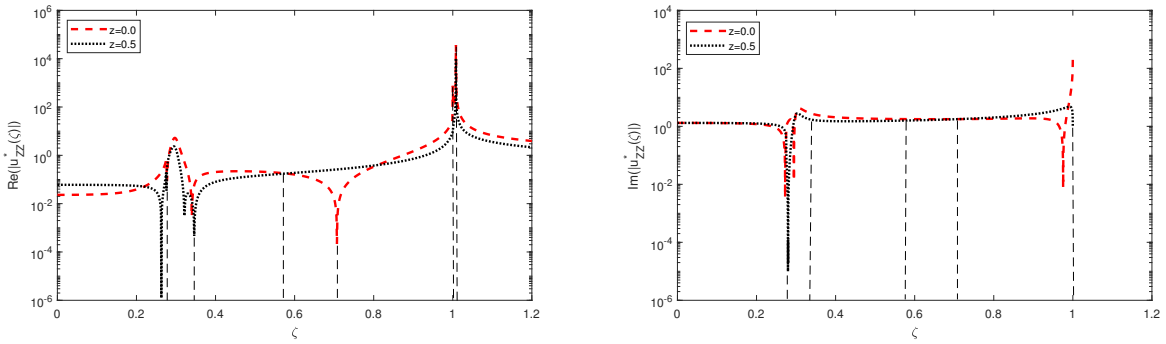

Figura 3 – Location of all singularities for present case

Figure 3 shows dashed vertical lines where the singularities are predicted to occur. This figure is merely illustrative, as not all singularities can be represented graphically. Moreover, since logarithm graphs can only show the absolute of the function, some points that appear as singularities in the graph are in fact points where the function is zero; it is merely changing sign. The evaluation of the integrand at ζ' confirms the presence of the singularities at the predicted locations.

Notice that the absence of an imaginary component after $\zeta = 1$ indicates that the integrand is purely real after that point. After this point, the integrand is free of singularities, and an oscillatory-decaying aspect dominates its behavior, as it has been shown and treated by the authors through extrapolation methods (Cavalcante and Labaki, 2018 and 2019; Cavalcante, Vasconcelos and Labaki, 2017). The confidence that the singularities fall within $\zeta < 1$ is only possible due to the normalization of the integration variable from λ' to $\zeta = \lambda'/\delta$ (see Eq. (1)) proposed by Rajapakse and Wang (1993).

Note that one is only able to make such assertion on the physical correlation of the singularities for integrals with some physical significance, such as the present one chances to be. For general, purely abstract singular integrals, one needs to resort to numerical methods to locate the singularities (e.g., Rizzardi, 2018).

CONCLUSION

This works investigated the localization of singularities that occur in the integrand of Green's functions for multilayered half-spaces. Differently than the case of homogeneous half-spaces, there is no closed-form expression for the location

of the singularities for the case of layered systems. There is, however, a direct correspondence between the physical wavenumbers of each layer and the singularities in the integrand. These provide reliable points where the integration interval can be divided for its subsequent integration through some appropriate method.

ACKNOWLEDGEMENTS

The research leading to this article has been funded in part by the São Paulo Research Foundation - Fapesp, through grant 2017/01450-0. The support of Capes, CNPq, and Faepex-Unicamp is also gratefully acknowledged.

APPENDIX

This appendix lists the parameters appearing in Eqs. (2) and (3), for $i = 1, 2$,

$$b_{2i} = [\alpha\delta^2\xi_i^2 - (\kappa - 1)\delta^2\zeta^2\vartheta_i]J_0(\delta\zeta r) \tag{16}$$

$$\frac{a_7}{\delta\xi_1} = \frac{a_8}{\delta\xi_2} = J_0(\delta\zeta r) \tag{17}$$

$$\frac{a_i}{\vartheta_i} = \frac{b_{5i}}{(1+\vartheta_i)\delta^2\xi_i} = -\delta^2\xi_i J_1(\delta\zeta r) \tag{18}$$

In Eqs. (16) to (18), J_m is the Bessel function of the first kind and m^{th} order and

$$\vartheta_{1,2} = \frac{\alpha\xi_{1,2}^2 - \zeta^2 + 1}{\kappa\zeta^2} \tag{19}$$

$$\xi_{1,2} = \frac{1}{\sqrt{2\alpha}}(\gamma\zeta^2 - 1 - \alpha \pm \sqrt{\Phi})^{\frac{1}{2}} \tag{20}$$

$$\Phi = (\gamma\zeta^2 - 1 - \alpha)^2 - 4\alpha(\beta\zeta^4 - \beta\zeta^2 - \zeta^2 + 1) \tag{21}$$

$$\alpha = \frac{c_{33}}{c_{44}}, \quad \beta = \frac{c_{11}}{c_{44}}, \quad \kappa = \frac{c_{13} + c_{44}}{c_{44}}, \quad \delta^2 = \frac{\rho\omega^2}{c_{44}} \quad \text{and} \quad \gamma = 1 + \alpha\beta - \kappa^2 \tag{22}$$

where δ is a normalized frequency of excitation, ω is the frequency of excitation, and c_{ij} are elastic contants of the transversely isotropic material.

REFERENCES

Azevedo, A. C. V., Cavalcante, I., and Labaki, J., 2017, "On the Accuracy of Adaptive Quadratures in the Numerical Integration of Singular Green's Functions for Layered Media", In Proceedings of the XXXVIII Iberian Latin-American Congress on Computational Methods in Engineering - CILAMCE 2017, Florianopolis, Brazil.

Barros, P. L. A., 1996, "Elastodinâmica de Meios Transversalmente Isotrópicos: Funções de Green e o Método dos Elementos de Contorno na Análise da Interação Solo-estrutura", PhDthesis, University of Campinas, Campinas.

Cavalcante, I., and Labaki, J., 2019, "An FFT-based Generalization of the ε-algorithm for the Integration of Oscillatory-Ddecaying Functions with Multiple Frequencies", in Proceedings of the XV International Symposium on Dynamic Problems of Mechanics.

Cavalcante, I., and Labaki, J., 2018, "An Extension of Longmanś Method for the Integration of Beating, Oscillatory-Decaying Functions. In: United States National Congress for Applied and Theoretical Mechanics.

Cavalcante, I., Vasconcelos, A. C. A., and Labaki, J., 2017, A continuation algorithm-Longman's method scheme for the integration of transcendental functions. In: Iberian Latin American Congress on Computational Methods in Engineering.

Labaki, J., Mesquita, E. and Rajapakse, R. K. N. D., 2014, "Vertical Vibrations of an Elastic Foundation with Arbitrary Embedment within a Transversely Isotropic, Layered Soil", Computer Modeling in Engineering and Sciences, Vol. 103, pp. 281-313.

Rajapakse, R. K. N. D. and Wang. Y., 1993 "Green's Functions for Transversely Isotropic Elastic Half Space". Journal of Engineering Mechanics, 119, No. 9, pp. 1724-1746.

Rizzardi, M., 2018. Detection of the singularities of a complex function by numerical approximations of its Laurent coefficients. Numerical Algorithms, 77(4), pp.955-982.

Wang, Y., and Rajapakse, R.K.N.D., 1994. "An exact stiffness method for elastodynamics of a layered orthotropic half-plane". Journal of applied mechanics, 61(2), pp.339-348.

RESPONSIBILITY NOTICE

The authors are the only responsible for the printed material included in this paper.